Physics Letters B 751 (2015) 215–219

Contents lists available at ScienceDirect

Physics Letters B

www.elsevier.com/locate/physletb

Magnetic field effect on charmonium formation in high energy nuclear collisions

Xingyu Guo [a], Shuzhe Shi [a], Nu Xu [b,c], Zhe Xu [a], Pengfei Zhuang [a,*]

[a] Physics Department, Tsinghua University and Collaborative Innovation Center of Quantum Matter, Beijing 100084, China
[b] Nuclear Science Division, Lawrence Berkeley National Laboratory, Berkeley, CA 94720, USA
[c] Key Laboratory of Quark and Lepton Physics (MOE) and Institute of Particle Physics, Central China Normal University, Wuhan 430079, China

ARTICLE INFO

Article history:
Received 25 June 2015
Received in revised form 14 October 2015
Accepted 14 October 2015
Available online 23 October 2015
Editor: W. Haxton

ABSTRACT

It is important to understand the strong external magnetic field generated at the very beginning of heavy ion collisions. We study the effect of the magnetic field on the anisotropic charmonium formation in Pb + Pb collisions at the LHC energy. The time dependent Schrödinger equation is employed to describe the motion of $c\bar{c}$ pairs. We compare our model prediction of the non-collective anisotropic parameter v_2 of J/ψ with CMS data at high transverse momentum.

It is widely accepted that the strongest magnetic field in nature can be generated in the early stage of relativistic heavy ion collisions. The peak magnitude of the field can reach $eB \sim 5m_\pi^2$ in Au + Au collisions at the Relativistic Heavy Ion Collider (RHIC) and $70m_\pi^2$ in Pb + Pb collisions at the Large Hadron Collider (LHC) [1–8], where e is the electron charge and m_π the pion mass. When the magnetic field survives in the hot medium, the interaction between the field and the medium may change the fundamental QCD topological structures [9] such as the chiral magnetic effect [10–13], the chiral magnetic wave [14–16], the chiral separation effect [13,17,18], the chiral vortical effect [17,19], the chiral electric separation effect [20], and the enhancement of elliptic flow of charged particles [21–23]. Recent experimental and theoretical results on particle production in electromagnetic fields in heavy ion collisions can respectively be found in Refs. [24] and [25].

While the magnetic field induced QCD chirality in hot medium is fundamentally interesting, the fast dropping of the initially created magnetic field is reduced by at least one–two orders of magnitude before the hot medium formation [6,9,25], and the strongest magnetic field is most probably only at the very beginning of nuclear collisions. So far, no experimental determination of this initial magnetic field has been made. In this Letter, we propose using the anisotropy parameters of high momentum charmonia to probe the initial magnetic field. While low momentum charmonia are produced through initial hard processes and later regeneration [26–29] and strongly suppressed by the medium [30], high momentum charmonia are created only in the initial stage. Except interaction with the magnetic field, which will be discussed here, the high momentum charmonia are not affected by the hot medium and therefore can be used as an ideal tool to probe the initial magnetic field in high energy nuclear collisions. Note, in this work we only focus on the magnetic field induced by the spectators in the initial stage, the effects of the QCD topological structures and anisotropic heavy quark potential [31] in the later stage will not change our main conclusions.

Considering the charmonium formation time $t_f \sim 0.5$ fm/c [32], the magnetic field at the very beginning will mainly affect the charmonium formation process from a $c\bar{c}$ pair to its bound state $\Psi = J/\psi, \psi', \chi_c, \cdots$ and could cause some profound effects on (i) Charmonium yields: the magnetic field induced force will change the charmonium fractions $|C_\Psi|^2$ in the $c\bar{c}$ pair $|c\bar{c}\rangle = C_\Psi|\Psi\rangle$ and thus alters the relative yields among different charmonium states, and (ii) Charmonium momentum distribution: the specific direction along the magnetic field breaks down the rotational symmetry of the system, which leads to an anisotropic charmonium production in the transverse plane. Both effects can be experimentally checked.

As charm quarks are heavy enough in comparison with the relative motion inside a charmonium which is determined by the J/ψ radius due to the uncertainty principle, $m_c \sim 1.3$ GeV $> p \sim 1/r \sim 1/0.5$ fm$^{-1} = 0.4$ GeV, we can ignore relativistic effects in considering the inner structure of a $c\bar{c}$ bound state. The charmonium energy E_Ψ and wave function $\Psi(\mathbf{r})$ are determined by the Schrödinger equation

$$\hat{H}_0\Psi = E_\Psi\Psi, \quad (1)$$

* Corresponding author.
E-mail address: zhuangpf@mail.tsinghua.edu.cn (P. Zhuang).

http://dx.doi.org/10.1016/j.physletb.2015.10.038

where $\hat{H}_0$ is the Hamiltonian of the $c\bar{c}$ bound state without magnetic field, including only the Cornell potential together with the spin–spin interaction [33],

$$V_f(r) = -\alpha/r + \sigma r + \beta e^{-\gamma r}\mathbf{s}_c \cdot \mathbf{s}_{\bar{c}}. \tag{2}$$

By fitting the charmonium spectrum in vacuum, one can fix the potential parameters as $m_c = 1.29$ GeV, $\sigma = 0.174$ GeV^2, $\alpha = 0.312$, $\beta = 1.982$ GeV and $\gamma = 2.06$ GeV.

The evolution of a $c\bar{c}$ pair state Φ into a charmonium state Ψ in a magnetic field is controlled by the time dependent Schrödinger equation

$$i\partial\Phi/\partial t = \hat{H}\Phi \tag{3}$$

with the Hamiltonian operator

$$\hat{H} = \left(\hat{\mathbf{p}}_c - q\mathbf{A}_c\right)^2/(2m_c) + \left(\hat{\mathbf{p}}_{\bar{c}} + q\mathbf{A}_{\bar{c}}\right)^2/(2m_c) + V_i, \tag{4}$$

where $\mathbf{A}$ is the magnetic potential, $q = 2e/3$ the charm quark electron charge, and V_i the $c\bar{c}$ potential. While V_i and V_f are both the potentials between c and $\bar{c}$, the former is for pre-bound states, and the latter is for bound states. The charmonium formation mechanism, or the concrete form of V_i has been widely discussed in literatures, see for instance Ref. [34]. By separating the $c\bar{c}$ wave function $\Phi(t, \mathbf{r}_c, \mathbf{r}_{\bar{c}})$ into a center-of-mass part and a relative part $\Phi = \Phi_R\Phi_r$ with the center-of-mass coordinator $\mathbf{R} = (\mathbf{r}_c + \mathbf{r}_{\bar{c}})/2$ and relative coordinator $\mathbf{r} = \mathbf{r}_c - \mathbf{r}_{\bar{c}}$, and further expanding the relative part in terms of the charmonium wave functions $\Psi(\mathbf{r})$,

$$\Phi = \frac{1}{\sqrt{2\pi}} e^{i\mathbf{P}_k\cdot\mathbf{R} - \frac{\mathbf{P}_p^2}{4m_c}t} \sum_\Psi C_\Psi e^{-iE_\Psi t}\Psi, \tag{5}$$

the probability $|C_\Psi(t)|^2$ for the $c\bar{c}$ pair to be in the charmonium state Ψ satisfies the evolution equation

$$\frac{d}{dt}C_\Psi = \sum_{\Psi'} e^{i(E_\Psi - E_{\Psi'})t} C_{\Psi'} \int d^3\mathbf{r}\Psi^*(\mathbf{r})\hat{H}'\Psi'(\mathbf{r}) \tag{6}$$

with

$$\hat{H}(t) = \hat{H}_0 + \hat{H}'(t), \qquad \hat{H}'(t) = \hat{H}_B(t) + V_i - V_f,$$
$$\hat{H}_B(t) = -\boldsymbol{\mu}\cdot\mathbf{B} - \frac{q}{2m_c}(\hat{\mathbf{P}}_p \times \mathbf{B})\cdot\mathbf{r} + \frac{q^2}{4m_c}(\mathbf{B}\times\mathbf{r})^2. \tag{7}$$

In deriving the magnetic field term $\hat{H}_B(t)$, we have used the relation $\mathbf{B} = \nabla\times\mathbf{A}$ and a special choice $\mathbf{A} = (Bz/2, 0, -Bx/2)$ which leads to a constant magnetic field $\mathbf{B} = B\mathbf{e}_y$ along the y-axis.

Since we introduced a special direction, the direction of $\mathbf{B}$, the kinetic momentum $\mathbf{P}_k = \mathbf{P} - q(\mathbf{A}_c - \mathbf{A}_{\bar{c}})$ with the total momentum $\mathbf{P} = \mathbf{p}_c + \mathbf{p}_{\bar{c}}$ is no longer conserved. The conserved part is the pseudo momentum $\mathbf{P}_p = \mathbf{P} + q(\mathbf{A}_c - \mathbf{A}_{\bar{c}})$ [35]. The $c\bar{c}$ pair interaction with the magnetic field is manifested by the three terms in $\hat{H}_B$: the first term is the spin-field interaction with the spin magnetic moment $\boldsymbol{\mu} = q/m_c(\mathbf{s}_c - \mathbf{s}_{\bar{c}})$, the second term comes from the Lorentz force which is proportional to the $c\bar{c}$ momentum, and the third term is the harmonic potential which is quadratic in $q\mathbf{B}$ and therefore its effect is much smaller in comparison with the first and second terms which are linear in $q\mathbf{B}$. At high momentum, the Lorentz force is the dominant magnetic field effect. Note that the spin-field interaction makes the spin angular momentum no longer a conserved quantity, the spin singlet η_c will couple with one of the triplet J/ψ which carries a zero spin component along the magnetic field $s_B = 0$ [35,36]. On the other hand, the Lorentz force and the harmonic potential break the rotational symmetry in the coordinate space.

Let us take the nuclear colliding direction as the z-axis and the impact parameter $\mathbf{b}$ parallel to the x-axis. While the created magnetic field in heavy ion collisions depends on the events, and the magnitude and direction fluctuate in space and time [1–6,8], we consider here an averaged magnetic field $\mathbf{B}$ in the space–time region determined by the colliding energy and the nuclear geometry,

$$\mathbf{B} = \begin{cases} B\mathbf{e}_y, & 0 < t < t_B,\ \frac{x^2}{(R_A - b/2)^2} + \frac{y^2}{(b/2)^2} + \frac{\gamma_c^2 z^2}{(b/2)^2} < 1, \\ 0, & \text{others}. \end{cases} \tag{8}$$

For Pb + Pb collisions with centrality 40% at $\sqrt{s_{NN}} = 2.76$ TeV, the geometry parameters and the Lorentz factor are fixed to be $R_A = 6.6$ fm, $b = 8$ fm and $\gamma_c = 1400$. From the MC simulation [6] at LHC, the initial magnetic field is very strong but decays away quickly. As an average, we take here the magnitude and life time of the magnetic field $eB = 25m_\pi^2$ and $t_B = 0.2$ fm/c.

In general case electromagnetic interaction is much weaker than strong interaction and is often neglected in the study of QCD. However, for the strongest magnetic field in nature generated in the early stage of high energy nuclear collisions, the case is totally different. Let us compare the linear potential in V_f and the Lorentz force in $\hat{H}_B$. From the parameters shown above and taking the high charmonium momentum $P = 10$ GeV/c, the ratio of the strengths of the two terms $\sigma/(qBP/(2m_c)) \sim 10^{-1}$ means only a contribution of 10^{-2} from the strong interaction to the probability $|C_\Psi|^2$. The magnetic field effect here is similar to the temperature or density effect which significantly changes the strong interaction and controls the QCD phase transitions at finite temperature and density. Considering this small ratio, the potentials V_i and V_f and in turn the difference $V_i - V_f$ in Eq. (7) can safely be neglected when a strong magnetic field is introduced, and we can take the approximation $\hat{H}' = \hat{H}_B$.

To solve the dynamical equation (6) for the probability magnitude $C_\Psi(t)$, we need the initial value $C_\Psi(0)$ or the initial wave function $\Phi_r(0)$. Suppose the relative motion of the $c\bar{c}$ pair is initially described by a compact Gaussian wave package

$$\Phi_r(0) \sim e^{-\frac{(\mathbf{r}-\mathbf{r}_0)^2}{\sigma_0^2}}. \tag{9}$$

Since the azimuth angles of the averaged relative coordinate $\mathbf{r}_0 = r_0(\sin\theta_0\cos\phi_0, \sin\theta_0\sin\phi_0, \cos\theta_0)$ are randomly distributed before the magnetic field is introduced, we should do ensemble average over θ_0 and ϕ_0 in the final state. The remaining two parameters r_0 and σ_0 can be fixed by fitting the charmonium fractions in p + p collisions where there is no magnetic field. Inspired from the repulsive interaction between the c and $\bar{c}$, an initial point-like wave function $\delta(\mathbf{r}-\mathbf{r}')$ is supposed to develop as $e^{-(\mathbf{r}-\mathbf{r}')^2/(v^2t^2)}$ with a constant expansion velocity v. Therefore, the initial Gaussian wave package evolves as

$$\Phi_r(t) \sim \int d^3\mathbf{r}' e^{-\frac{(\mathbf{r}'-\mathbf{r}_0)^2}{\sigma_0^2}} e^{-\frac{(\mathbf{r}-\mathbf{r}')^2}{v^2t^2}} \sim e^{-\frac{(\mathbf{r}-\mathbf{r}_0)^2}{\sigma_t^2}}. \tag{10}$$

It is still a Gaussian wave package but with a time dependent width $\sigma_t^2 = \sigma_0^2 + v^2t^2$. Calculating the probability $|C_\Psi(t)|^2 = |\langle\Psi|\Phi_r(t)\rangle|^2$ and taking the experimentally observed decay branch ratios $\mathcal{B}(\Psi \to J/\psi)$ [37], we obtain the J/ψ fractions from direct production and feed down from the excited states,

$$R_\Psi(t) = \frac{|C_\Psi(t)|^2\mathcal{B}(\Psi \to J/\psi)}{\sum_{\Psi'}|C_{\Psi'}(t)|^2\mathcal{B}(\Psi' \to J/\psi)} \tag{11}$$

with the definition of $\mathcal{B}(J/\psi \to J/\psi) = 1$. Taking $R_{J/\psi}(t_f) = 60\%$, $R_{\psi'}(t_f) = 10\%$ and $R_{\chi_c}(t_f) = 30\%$ from the recent p + p data at

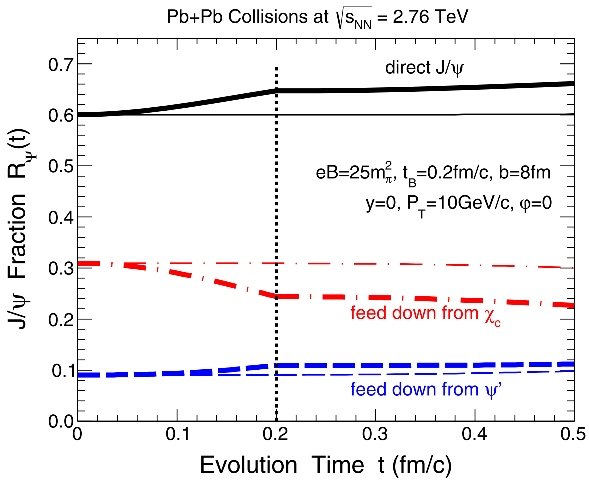

Fig. 1. (Color online.) The time evolution of J/ψ fractions for direct production (solid lines) and feed down from ψ' (dashed lines) and χ_c (dot-dashed lines). The thick and thin lines are the results with and without magnetic filed, respectively. As indicated by the vertical short-dashed line, the magnetic field only lasts during the time $t < t_B = 0.2$ fm/c.

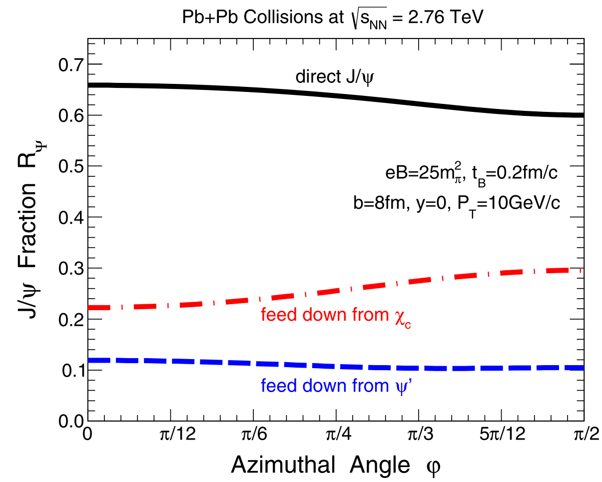

Fig. 2. (Color online.) The anisotropic J/ψ fractions R_Ψ in the transverse plane at the charmonium formation time $t_f = 0.5$ fm/c.

LHC energy [38–40] and the charmonium formation time $t_f = 0.5$ fm/c [32], we obtain $r_0 = 0.68$ fm and $\sigma_0 = 0.02$ fm, which correspond to the expansion velocity $v = 0.72$c and the final width $\sigma_{t_f} = 0.38$ fm.

With the known initial wave function $\Phi_r(0)$ or the initial probability magnitudes $C_{J/\psi}(0) : C_{\psi'}(0) : C_{\chi_c}(0) = 1 : 0.5 : 1.2$, we can solve the evolution equation (6) for $C_\Psi(t)$ in the time region $0 < t < t_B$ when the magnetic field is turned on. After that the wave function evolves according to the expansion rule (10) with $\Phi_r(t_B, \mathbf{r})$ as the initial condition,

$$\Phi_r(t, \mathbf{r}) \sim \int d^3\mathbf{r}' \Phi_r(t_B, \mathbf{r}') e^{-\frac{(\mathbf{r}-\mathbf{r}')^2}{v^2(t-t_B)^2}}, \qquad t > t_B. \tag{12}$$

We now show our numerical results for the magnetic field effect on the charmonium formation in heavy ion collisions. We focus on the central rapidity region in Pb + Pb collisions with impact parameter $b = 8$ fm at LHC energy $\sqrt{s_{NN}} = 2.76$ TeV. In the calculation, the initial $c\bar{c}$ pairs which are determined by the colliding energy and the nuclear geometry are assumed to be distributed homogeneously in the overlapping region of the two colliding nuclei. In solving the equation (6) for $C_\Psi(t)$, we take a cutoff in the sum over the charmonium eigenstate Ψ: the main quantum number $n \le 6$ and the orbital angular momentum number $l \le 7$. This choice guarantees the precise of 10^{-5} for the probabilities $|C_\Psi|^2$.

In Fig. 1, the J/ψ fractions $R_\Psi(t)$ from different channels are shown as functions of the $c\bar{c}$ evolution time at fixed transverse momentum $P_T = 10$ GeV/c. In case without considering the magnetic field (thin lines), the fractions are almost constants during the evolution. When the magnetic field is turned on (thick lines), the $c\bar{c}$ motion becomes anisotropic, we have fixed in Fig. 1 the $c\bar{c}$ azimuthal angle in the transverse plane $\varphi = \arctan(P_y/P_x) = 0$ where the magnetic field effect is expected to be the strongest. In the time period $t < t_B$, the external magnetic field serves as a stimulator that enhances the quantum mechanics allowed transition from χ_c to J/ψ and ψ' and from ψ' to J/ψ. After the field is off at $t > t_B$, the variation of all the fractions with time becomes mild again. At the formation time $t_f = 0.5$ fm/c, the relative enhancements for both direct J/ψ production and feed down from ψ' are found to be 10%, and the contribution from χ_c decay is relatively suppressed by 23%.

Having discussed the different contributions to J/ψ production, we now look at the yields for J/ψ, ψ' and χ_c. For J/ψ, the ratio between the yields $N^{(B)}_{J/\psi}$ and $N^{(0)}_{J/\psi}$ with and without the magnetic field can be expressed in terms of the probabilities $|C^{(B)}_\Psi(t_f)|^2$ and $|C^{(0)}_\Psi(t_f)|^2$ and the fractions $R^{(0)}_\Psi(t_f)$,

$$\frac{N^{(B)}_{J/\psi}(t_f)}{N^{(0)}_{J/\psi}(t_f)} = \frac{\sum_\Psi |C^{(B)}_\Psi(t_f)|^2 \mathcal{B}(\Psi \to J/\psi)}{\sum_\Psi |C^{(0)}_\Psi(t_f)|^2 \mathcal{B}(\Psi \to J/\psi)} = \sum_\Psi \frac{|C^{(B)}_\Psi(t_f)|^2}{|C^{(0)}_\Psi(t_f)|^2} R^{(0)}_\Psi(t_f). \tag{13}$$

Using the above calculated probabilities and fractions at LHC energy, the maximum J/ψ enhancement at $\varphi = 0$ and $P_T = 10$ GeV/c is 13%. For the excited states, neglecting the feed down from the higher eigenstates of $\hat{H}_0$, we have the yield ratios $N^{(B)}_{\psi'}(t_f)/N^{(0)}_{\psi'}(t_f) = 1.29$ for ψ' and $N^{(B)}_{\chi_c}(t_f)/N^{(0)}_{\chi_c}(t_f) = 0.84$ for χ_c, which mean, due to the magnetic field, a relative enhancement of 29% for ψ' and suppression of 16% for χ_c.

Fig. 2 shows the magnetic field induced anisotropic J/ψ fractions $R_\Psi(t_f)$ at fixed transverse momentum $P_T = 10$ GeV/c. The strength of the Lorentz force acting on the $c\bar{c}$ pairs is most strong at $\varphi = 0$ and drops down monotonously with increasing azimuthal angle φ. Finally at $\varphi = \pi/2$, the force disappears and only the weak harmonic potential exists, and the fractions approach to their vacuum values.

We now show in Fig. 3 the magnetic field induced transverse momentum dependence of the J/ψ fractions $R_\Psi(t_f)$. We again fix the angle $\varphi = 0$ to see the maximum magnetic field effect. At $P_T = 0$ the Lorentz force disappears, the slight deviation of the fractions from the vacuum values comes from the weak harmonic potential. Since the strength of the Lorentz force is proportional to the $c\bar{c}$ pair momentum, the change of the fractions increases with P_T in the beginning. However, when the $c\bar{c}$ pairs move very fast, the time they experienced in the magnetic field may become shorter than the life time t_B of the magnetic field. This leakage effect leads to the saturation of the fractions at high transverse momentum, shown in Fig. 3.

Usually, the observed anisotropy v_2 is discussed in the framework of hydrodynamics, representing the collective motion of the medium [41–43]. At LHC, J/ψ v_2 has been reported in the region of $P_T < 10$ GeV/c [44]. Since the collective motion is dominated by the bulk interactions in relatively low momentum region, those high P_T charmonia generated in the initial stage are not expected to be sensitive to the nature of the hot medium. However,

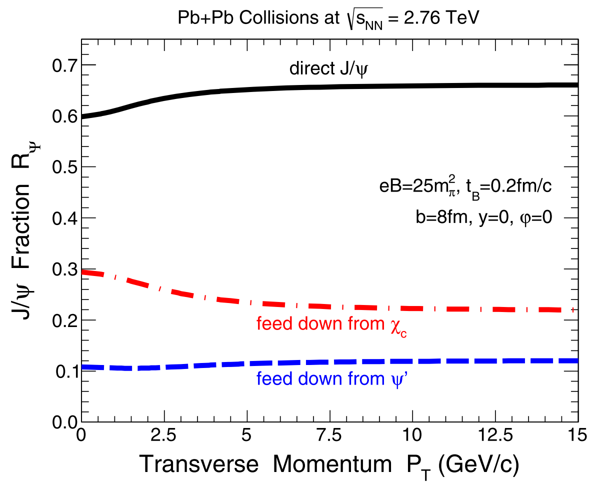

Fig. 3. (Color online.) The transverse momentum dependence of the J/ψ fractions R_ψ at the charmonium formation time $t_f = 0.5$ fm/c.

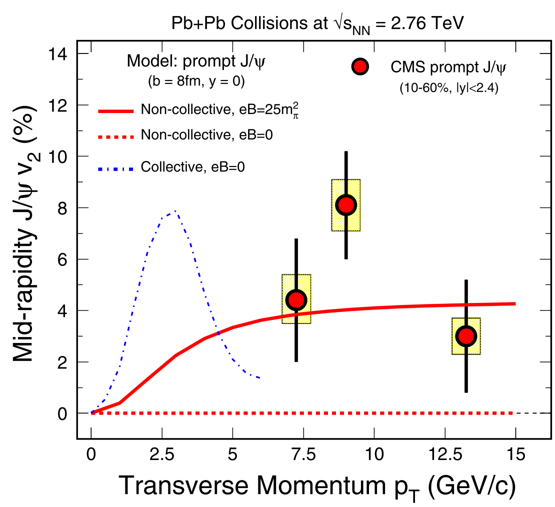

Fig. 4. (Color online.) The transverse momentum dependence of J/ψ v_2. The solid and dashed lines are the non-collective J/ψ v_2 at charmonium formation time $t_f = 0.5$ fm with and without magnetic field, and the data at high P_T are from the CMS Collaboration [45]. As a comparison, the collective J/ψ v_2 from a transport model [41] is shown as the dot-dashed line.

the Lorentz force induced anisotropic production in the transverse plane, shown in Fig. 2, may result in a non-collective J/ψ v_2 at high P_T. The J/ψ v_2 as a function of rapidity and transverse momentum is defined as

$$v_2(\eta, P_T) = \frac{\int_0^{2\pi} N_{J/\psi}(\eta, P_T, \varphi)\cos(2\varphi)d\varphi}{\int_0^{2\pi} N_{J/\psi}(\eta, P_T, \varphi)d\varphi}. \quad (14)$$

The numerical result is shown in Fig. 4. In calculation without magnetic field [41–43], the initial J/ψs are isotropically produced with $v_2 = 0$ (dashed line). However, due to the Lorentz force, the high P_T J/ψs acquire sizable non-collective v_2 (solid line), which explains reasonably well the CMS data [45] for prompt J/ψs in the high P_T region. As a comparison, we show in Fig. 4 also the collective v_2 (dot-dashed line) calculated from a dynamical transport model [41]. Different from the collective flow which comes from the J/ψ regeneration at low and intermediate P_T, the non-collective v_2 induced by the magnetic field is mainly in high P_T region. As one can see in Figs. 1, 2 and 3, the J/ψ and ψ' enhancement is accompanied by the χ_c suppression. Hence it is interesting to point out that if the observed non-collective v_2 for J/ψ is positive, the high P_T v_2 for χ_c should be negative. One should note that the magnetic field effect on charmonium production before the quark gluon plasma formation is probably not the only source for J/ψ elliptic flow at high P_T. For instance, the path length difference in non-central heavy ion collisions will introduce finite non-collective anisotropy, see discussions in [46] and references therein. On the other hand, the anisotropy of the quark gluon plasma in the early stage leads to anisotropic distribution of high P_T gluons, and therefore, those J/ψs from the gluon fragmentation carry anisotropic transverse momentum. Since the absorption of the gluons in-plane should be weaker than out-of-plane, the elliptic flow of these J/ψs is positive too. However, by comparing with the elliptic flow of the excited state χ_c, one may distinguish between these mechanisms. If the flow is induced by the initial magnetic field, χ_c should have negative v_2, as we emphasized above. If the flow is resulted from the path length difference or anisotropic fragmentation, χ_c should have positive v_2 too. A combined analysis of the non-collective v_2, originated from the more conventional source and the novel mechanism put forward in this Letter, will be important and necessary for a quantitatively determination on the strength of the magnetic field.

In summary, the strongest magnetic field at the very beginning of high energy nuclear collisions affects mainly the charmonium formation process. As a consequence, the relative yields between different charmonium states are sizeably changed and the charmonium production becomes anisotropic. By solving the time dependent Schrödinger equation for the $c\bar{c}$ pairs, we studied the effect of the initially created magnetic field on the charmonium yields and momentum distributions in Pb + Pb collisions at LHC. We found (i) the directly produced and ψ' decayed J/ψs are enhanced by 13% and 29%, respectively, while the χ_c decayed J/ψs are suppressed by 16%, and (ii) the non-collective J/ψ v_2 at large transverse momentum, $P_T \geq 8$ GeV/c, is as large as 4% and comparable with the CMS data, while the χ_c v_2 becomes negative in the high P_T region. We wish to point out that in high energy nuclear collisions the initial magnetic field is related to several important measurements reflecting the intrinsic structure of the QCD. The measurement of a J/ψ anisotropy at large P_T can be used to diagnose the magnetic filed in such collisions.

Acknowledgements

The work is supported by the NSFC (11275103, 11335005), MOST (2013CB922000, 2014CB845400, 2015CB856900) and DOE (DE-AC03-76SF00098).

References

[1] J. Rafelski, B. Müller, Phys. Rev. Lett. 36 (1976) 517.
[2] V. Skokov, A. Illarionov, V. Toneev, Int. J. Mod. Phys. A 24 (2009) 5925.
[3] M. Asakawa, A. Majumder, B. Müller, Phys. Rev. C 81 (2010) 064912.
[4] V. Voronyuk, et al., Phys. Rev. C 83 (2011) 054911.
[5] L. Ou, B. Li, Phys. Rev. C 84 (2011) 064605.
[6] W. Deng, X. Huang, Phys. Rev. C 85 (2012) 044907.
[7] B.G. Zakharov, Phys. Lett. B 737 (2014) 262.
[8] Y. Liu, C. Greiner, C. Ko, arXiv:1403.4317.
[9] U. Gürsoy, D. Kharzeev, K. Rajagopal, Phys. Rev. C 89 (2014) 054905.
[10] A. Vilenkin, Phys. Rev. D 22 (1980) 3080.
[11] M. Metlitshi, A. Zhitnitsky, Phys. Rev. D 72 (2005) 045011.
[12] G. Newman, D. Son, Phys. Rev. D 73 (2006) 045006.
[13] D. Kharzeev, L. McLerran, H. Warringa, Nucl. Phys. A 803 (2008) 227.
[14] D. Kharzeev, H. Yee, Phys. Rev. D 83 (2011) 085007.
[15] E. Gorbar, V. Miransky, I. Shovkovy, Phys. Rev. D 83 (2011) 085003.
[16] Y. Burnier, D. Kharzeev, J. Liao, H. Yee, Phys. Rev. Lett. 107 (2011) 052303.
[17] D. Kharzeev, A. Zhitnitsky, Nucl. Phys. A 797 (2007) 67.
[18] K. Fukushima, D. Kharzeev, H. Warringa, Phys. Rev. D 78 (2008) 074033.
[19] D. Kharzeev, D. Son, Phys. Rev. Lett. 106 (2011) 062301.

[20] X. Huang, J. Liao, Phys. Rev. Lett. 110 (2013) 232302.
[21] K. Tuchin, J. Phys. G 39 (2012) 025010.
[22] G. Basar, D. Kharzeev, V. Skokov, Phys. Rev. Lett. 109 (2012) 202303.
[23] G. Basar, D. Kharzeev, E. Shuryak, Phys. Rev. C 90 (2014) 014905.
[24] N. Xu, STAR Collaboration, Nucl. Phys. A 931 (2014) 1c;
F. Zhao, STAR Collaboration, Nucl. Phys. A 931 (2014) 746c;
Q. Shou, STAR Collaboration, Nucl. Phys. A 931 (2014) 758c.
[25] K. Tuchin, Adv. High Energy Phys. 2013 (2013) 490495.
[26] P. Braun-Munzinger, J. Stachel, Phys. Lett. B 490 (2000) 196.
[27] L. Grandchamp, R. Rapp, Nucl. Phys. A 709 (2002) 415.
[28] R.L. Thews, M.L. Mangano, Phys. Rev. C 73 (2006) 014904.
[29] L. Yan, P. Zhuang, N. Xu, Phys. Rev. Lett. 97 (2006) 232301.
[30] T. Matsui, H. Satz, Phys. Lett. B 178 (1986) 416.
[31] C. Bonati, M. D'Elia, M. Mariti, M. Mesiti, F. Negro, Phys. Rev. D 89 (2015) 114502.
[32] C. Gerschel, J. Huefner, Annu. Rev. Nucl. Part. Sci. 49 (1999) 255.
[33] T. Kawanai, S. Sasaki, Phys. Rev. D 85 (2012) 091503.
[34] D. Kharzeev, H. Satz, Phys. Lett. B 366 (1996) 316.
[35] J. Alford, M. Strickland, Phys. Rev. D 88 (2013) 105017.
[36] D. Yang, B. Müller, J. Phys. G 39 (2012) 015007.
[37] K. Olive, et al., Particle Data Group, Chin. Phys. C 38 (2014) 090001.
[38] ATLAS Collaboration, J. High Energy Phys. 07 (2014) 154.
[39] CMS Collaboration, J. High Energy Phys. 02 (2012) 011.
[40] LHCb Collaboration, Eur. Phys. J. C 72 (2012) 2100.
[41] K. Zhou, N. Xu, Z. Xu, P. Zhuang, Phys. Rev. C 89 (2014) 054911.
[42] X. Zhao, A. Emerick, R. Rapp, Nucl. Phys. A 904–905 (2013) 611c.
[43] R. Katz, P. Gossiaux, J. Phys. Conf. Ser. 509 (2014) 012095.
[44] E. Abbas, et al., ALICE Collaboration, Phys. Rev. Lett. 111 (2013) 162301.
[45] CMS Collaboration, CMS PAS HIN-12-001.
[46] J.C. Xu, J.F. Liao, M. Gyulassy, arXiv:1411.3673.